First published in
SURFACE AND INTERFACE ANALYSIS
Surf. Interface Anal. 2006; **38**: 1090–1095
Published online 24 April 2006 in Wiley InterScience
(www.interscience.wiley.com) DOI: 10.1002/sia.2321

Finite element analysis of V-shaped cantilevers for atomic force microscopy under normal and lateral force loads

Matthias Müller,[1]* Thomas Schimmel,[1,2] Pascal Häußler,[3] Heiko Fettig,[3] Ottmar Müller[3] and Albert Albers[3]

[1] Institute of Applied Physics, University of Karlsruhe, D-76128 Karlsruhe, Germany
[2] Institute of Nanotechnology (INT), Forschungszentrum Karlsruhe, D-76021 Karlsruhe, Germany
[3] Institute of Product Development (IPEK), University of Karlsruhe, D-76128 Karlsruhe, Germany

Received 24 June 2005; Revised 17 August 2005; Accepted 22 August 2005

For the quantitative investigation of surface properties such as elasticity, friction and wear by atomic force microscopy (AFM), a quantitative determination of the forces acting on the probe during its motion along the sample surface is essential. In this article, a fully parameterized finite element model for V-shaped cantilevers is presented and the three-dimensional mechanical deformations of the AFM cantilever are investigated. Force constants and detection angles for tip displacements in the three spatial directions are calculated for widely used cantilevers. The limits of linearity according to Hook's law are studied. It is found that the AFM contact cantilevers investigated here show a linear bending behavior for tip displacements within a range below approx. 10 nm in lateral directions and 100 nm in the normal direction. Displacements within this range are typical for many AFM applications including force modulation techniques. For higher loads as used e.g. for surface modification, a significant deviation from linear behavior is observed. Copyright © 2006 John Wiley & Sons, Ltd.

KEYWORDS: atomic force microscopy; AFM; cantilevers; force constant; force calibration; elastic properties; tribology; scanning probe microscopy

INTRODUCTION

Atomic force microscopy (AFM), apart from topographical imaging, also allows the investigation of mechanical properties of surfaces, with high lateral resolution down to the nanometer scale. By using special modes of operation such as lateral force microscopy (LFM), atomic force acoustic microscopy (AFAM) or force-modulated microscopy (FMM), it is possible to obtain spatially resolved tribological and elastic properties of the contact between the sample and the AFM probe.[1–3] Moreover, the AFM tip can also be used for the study of adhesion and wear as well as for the modification of the sample surface on the nanometer scale.[4–6] For each of the methods mentioned above, lateral forces – which means forces acting parallel to the sample surface – play an important role.

For the interpretation of the AFM data and in order to perform a quantitative analysis of such measurements, it is necessary to quantify the mechanical deformations of the cantilever due to normal forces as well as due to lateral forces. This implies that the detection sensitivities and, in particular, the different force constants of the AFM cantilever for tip displacements in the three spatial directions must be known. Furthermore, the limits of applicability of these data should also be known.

However, usually in cantilever data sheets, in addition to the first eigenfrequency of the cantilever, only the force constant for tip displacement perpendicular to the plane of the cantilever (bending force constant) is found. Moreover, the measurement of the bending force constant is more feasible than that of the force constants for tip displacements in the lateral directions.[7] Therefore, there is a need for calculations to obtain the latter.

In contrast to the analytical calculations for rectangular cantilevers, the corresponding calculations for the widely used V-shaped cantilevers (Fig. 1) are not easily performed. Nevertheless, some analytical expressions are found in the literature,[8–14] which are useful for further discussions.[15,16] However, these approaches use a simplified V-shaped cantilever geometry (e.g. neglecting the triangular plate between the beam ends, Fig. 1). In several publications only the force constant for the normal direction is given,[8–10] and an expression for the torsional force constant is found only in some works.[11,12] The buckling force constant – which means the lateral force constant for tip displacement parallel to the cantilever axis – is rarely quoted. Neumeister *et al.*[13] have derived extensive analytic expressions for force constants of a simplified V-shaped cantilever geometry for the three fundamental directions of tip displacements,

*Correspondence to: Matthias Müller, Institute of Applied Physics, University of Karlsruhe, D-76128 Karlsruhe, Germany.
E-mail: matthias.mueller@physik.uni-karlsruhe.de

Surface and Interface Analysis

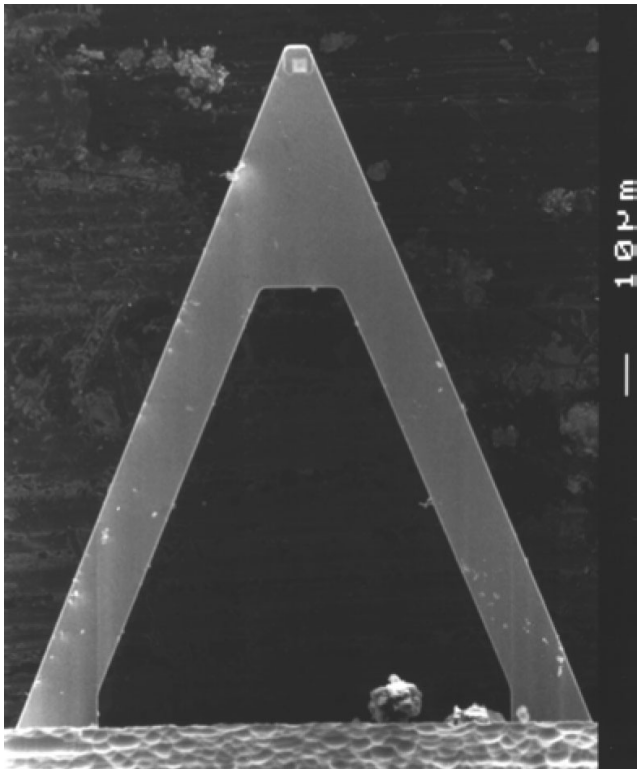

Figure 1. Image obtained by scanning electron microscopy (SEM) showing the V-shaped cantilever Microlever type C.

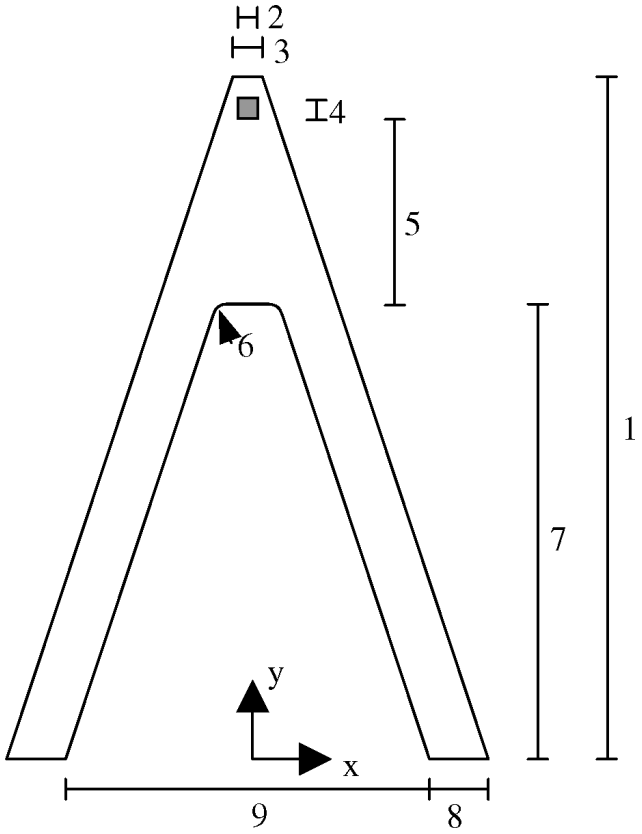

Figure 2. Geometrical parameters used for FE modeling. The parameters are listed in Table 1.

which are rather complicated. An analytical approach to calculate the force constant and detection sensitivity for tip displacements in the direction parallel to the cantilever axis has been given by Warmack *et al*.[14] Using a combination of finite element analysis (FEA) and resonance frequency measurements, Hazel *et al*.[12] proposed to determine the normal force constant and the torsional force constant. However, a publication containing all the necessary data mentioned above, as well as a more detailed discussion of the applicability of these data considering finite tip displacements, to our knowledge, is not yet available.

In this article, we present a fully parameterized FE model for V-shaped cantilevers. Force constants as well as detection sensitivities for tip displacements in the three fundamental directions are calculated for some widely used and commercially available cantilever geometries. The limits of the validity of Hook's law are discussed.

MODEL

For the FE modeling and analysis described in this article, the standard FEA software MSC.Nastran (solver) and MSC.Patran (pre-/post-processor) were used.

In order to calculate the mechanical properties for a variety of cantilevers with different geometric shapes and sizes, a parameterized FE model has been developed. The geometry is completely characterized by a set of parameters supplied by the user (Fig. 2 and Table 1). These parameters are stored in a model setup file and follow the MSC.Patran Command Language. The modeling runs without user interaction and results in a complete FE model of the cantilever (Fig. 3), ready for the analysis with MSC.Nastran. This allows a convenient investigation of V-shaped cantilevers with different geometrical parameters.

The FE model of the cantilever is composed of 3222 finite elements and 4011 nodes. The mesh of element boundaries is shown in Fig. 3. Owing to the fact that the thickness of the cantilever is much smaller than its length, the so-called shell elements (CQUAD4) were used for the modeling of the cantilever beam. In order to obtain correct results, the length-to-thickness ratio of the shell elements should not be smaller than certain limits. However, for the automatic geometry modeling and automatic meshing, relatively small elements are necessary. To verify the correct operation of this automatically generated model, the quality of the FE analysis results was tested against the results of a hand-made model with a coarse grain mesh in which the elements were closer to their ideal dimensions.

To consider a fully rigid attachment of the cantilever to its support, all translational and rotational degrees of freedom of the nodes at the end of both cantilever legs were constrained.

The cantilever tip was modeled with a rigid-bar element (RBE2) since the tip is stiff as compared to the cantilever beam. The RBE2 connects a single node representing the end of the tip rigidly to all nodes on the base plane of the tip. In doing so, the tip and also its base plane are assumed to be infinitely rigid. The applicability of this simplification was tested by a model containing a tip modeled with 3D solid elements. For obtaining correct results in dynamic

DOI: 10.1002/sia

Surface and Interface Analysis

Table 1. Top: force constants and detection sensitivities calculated by finite element analysis for different types of AFM cantilevers (Microlevers, type C, D, E, F). Bottom: geometrical parameters of the cantilevers used for the calculations (see also illustrations in Fig. 2)

Microlever type		C	D	E	F
Force constants and detection sensitivities calculated with FEM					
k_{xx}	[N/m]	51.00	69.72	125.26	194.20
k_{yy}	[N/m]	94.82	121.01	210.76	323.13
k_{zz}	[N/m]	0.0274	0.0828	0.468	2.365
$k_{yz} = k_{zy}$	[N/m]	−1.322	−2.554	−8.217	−22.650
n_y	[deg/μm]	18.7	18.8	18.8	18.8
n_z	[deg/μm]	0.0031	0.0044	0.0102	0.0166
l_x	[deg/μm]	17.4	17.4	18.1	18.1
Eigenfrequencies calculated with FE modal analysis					
f_1	[kHz]	6.55	15.46	50.07	165.91
f_2	[kHz]	40.24	92.21	285.8	843.0
Geometric FEM parameters (numbers as illustrated in Fig. 2)					
Cantilever length (1)	[μm]	323.5	216.5	115.5	68.7
Tip width (2)	[μm]	4.2	4.2	4.2	4.2
Top width (3)	[μm]	5	5.4	5.5	5
Tip length (4)	[μm]	4.2	4.2	4.2	4.2
Tip position (5)	[μm]	84	82	43.5	40
Inner radius (6)	[μm]	2	2	2	2
Inner length (7)	[μm]	233	130	67.5	24
Brace width (8)	[μm]	20	19.2	15.6	16
Bottom width (9)	[μm]	173	104	82	34
Cantilever thickness	[μm]	0.6	0.6	0.6	0.6
Tip height	[μm]	3	3	3	3
Tip angle	[deg]	35	35	35	35

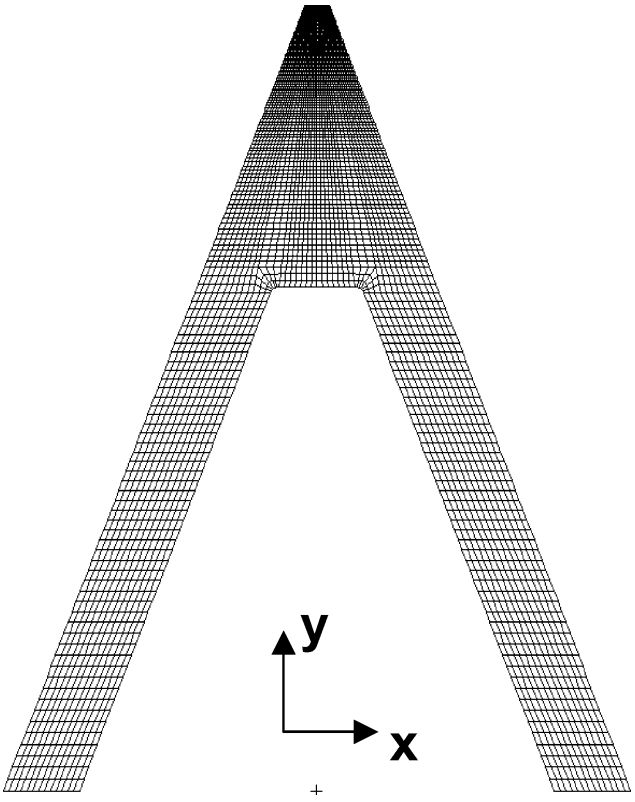

Figure 3. FE model of a V-shaped cantilever. The grid shows the boundaries of the elements.

solution sequences such as normal mode analysis, the mass of the tip is represented by a simple lumped-mass element.

The FE model was subsequently applied to analyze the properties of the widely used V-shaped silicon nitride contact-mode AFM cantilevers called Microlever. These cantilevers are commercially available from the supplier Veeco (Santa Barbara, USA) as cantilever types MLCT and MSCT. They are distributed on chips each of which provides six cantilevers of different geometries.

First, we focus on the calculations for the cantilever of type C. The geometric dimensions, which are illustrated in Fig. 2, were obtained from scanning electron microscopy (SEM) measurements (Fig. 1). Owing to variations of the production process, the effective Young's modulus and the thickness of the cantilever beam vary over a wide range. For this reason, typical values were used for our calculations (see below). An approach for more precise calculations for individual cantilevers is discussed later. Here, we consider an effective Young's modulus of 143 GPa and a Poisson's ratio 0.26. The thickness of the cantilever beam was assumed to be the nominal value of 0.6 μm given in the data sheet. The density of the cantilever beam was set to 3.2×10^{-15} kg/μm^3 as given in the literature.

To validate that the assumed parameters were reasonable, an FEM modal analysis was performed. We find that the calculated first FEM eigenfrequency is in good agreement

DOI: 10.1002/sia

with the resonance frequency of the cantilever given in the data sheet.

In a static analysis, loads were applied by enforced displacements of the tip in the three fundamental directions of the Cartesian frame of reference of the cantilever (x, y, z). The position of the cantilever tip without applied force loads defines the origin of the frame of reference, as shown in Fig. 4(a). The enforced displacements result in corresponding reaction forces $\vec{F}$ of the tip, which are calculated in order to get the force constant matrix $\overleftrightarrow{K}$ as a function of the displacement vector $\vec{r}$ solving the basic equation $d\vec{F} = -\overleftrightarrow{K}(r)d\vec{r}$. In addition, the unit vector with the direction normal to the base plane of the tip is determined. In this way, we were able to calculate the angles this plane rotates through along the x-axis and the y-axis respectively because of tip displacements (Fig. 4(b)). If the tip displacements are detected by laser beam deflection, as used in most AFM systems, the derivative of these angles as a function of the tip position can be used as a measure of the detection sensitivity of the tip displacements. With respect to the signals taken by AFM experiments, further factors have to be taken into account. These include the sensitivity of the photodiode or the distance between the point of laser reflection on the cantilever and the detector position. These factors are specific parameters for the AFM system being used and are not considered here. However, by considering the bending behavior of the cantilever and calculating the variation of the detection angles as a function of tip displacements, we are able to determine the *relative* detection sensitivities, which contain the complete effects of the cantilever deformation properties.

The calculations described above were carried out as a function of the enforced displacements of the tip in one direction, while the displacement in the perpendicular directions was fixed.

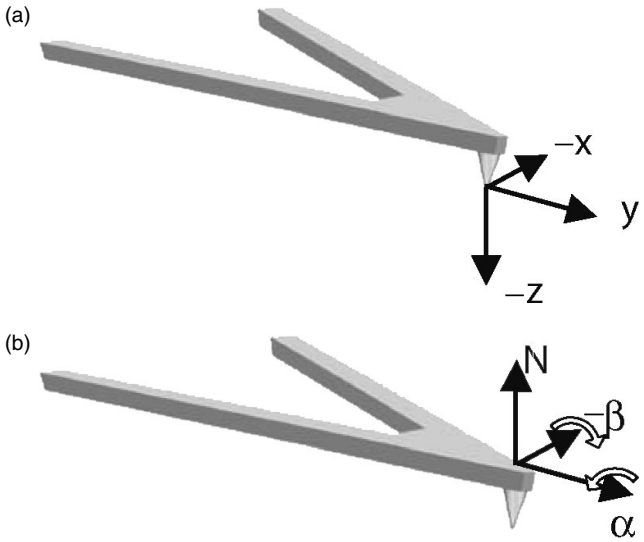

Figure 4. (a) The frame of reference used for FE analysis. (b) Illustration of the detection angles. The angles between the normal vector N of the base plane of the tip and the z direction are a measure of the deflection signals detected by the AFM. The torsion angle α corresponds to the lateral force signal and the bending angle β belongs to the normal force signal of a laser beam deflection in AFM.

RESULTS AND DISCUSSION

Limits of linearity

The results of the one-dimensional calculations for the Microlever type C are shown in Fig. 5. The graphs in Fig. 5(a–c) show the dependence of the nontrivial elements of the force constant matrix as a function of tip displacement (one diagram each for x, y and z displacements) with no displacements in the perpendicular directions. These elements were determined by the division of the change of the calculated reaction forces by the corresponding change of the applied tip displacement from one incremental calculation step to the next. For small tip displacements, the force constant elements are nearly constant. Therefore, within this regime the reaction forces of the tip show a linear dependence on the tip displacement according to the Hook's law. As shown in the graphs of Fig. 5(d–f) within this regime, the relative detection sensitivities, calculated as the change of the detection angles divided by the change of the position of the tip, are constant too, resulting in a linear detection behavior. In the graphs of (a) and (b) (and (d) and (e)) of Fig. 5 it is seen that this linear regime extends up to tip displacements of almost 10 nm in the lateral directions. For larger displacements, strong deviations from linearity occur owing to complex deformations of the entire cantilever. Since the corresponding lateral forces acting at these larger displacements are of the order of 1 μN and larger (using the force constant calculated above), the AFM, for typical loads, operates well within the linear regime with respect to lateral displacements. However, in the z direction (diagrams (c) and (f) of Fig. 5), a strong nonlinearity is observed for normal displacements larger than 100 nm, which corresponds to normal forces of the order of only 10 nN. In this regime of high z displacements, the normal force rises dramatically if no lateral displacement is allowed. The detection sensitivity shown in Fig. 5(c) also dramatically changes. Nevertheless, since many AFM measurements take place in the linear regime, this regime will now be discussed in more detail below.

3D description of force constants and detection sensitivities

Owing to the linear bending behavior of the cantilever in the linear regime shown above, force constants can be written as a constant matrix $\overleftrightarrow{K}$ and the relative detection sensitivities as constant vectors $\vec{\xi}_i$ in the frame of reference of the cantilever so that

$$\vec{F} = -\overleftrightarrow{K}\,\vec{r}, \quad \alpha = \vec{\xi}_{LFM}\,\vec{r}, \quad \beta = \vec{\xi}_{NFM}\,\vec{r} \qquad (1)$$

where $\vec{r}$ is the vector of tip displacement, $\vec{F}$ is the force acting at the tip, α is the torsion angle and β is the bending angle (Fig. 4(b)). As already discussed, α is a measure of the lateral force (LFM) signal, whereas β is a measure of the normal force (NFM) signal detected by the AFM. The force constant matrix $\overleftrightarrow{K}$ and the relative detection sensitivity vectors $\vec{\xi}_i$

DOI: 10.1002/sia

Surface and Interface Analysis

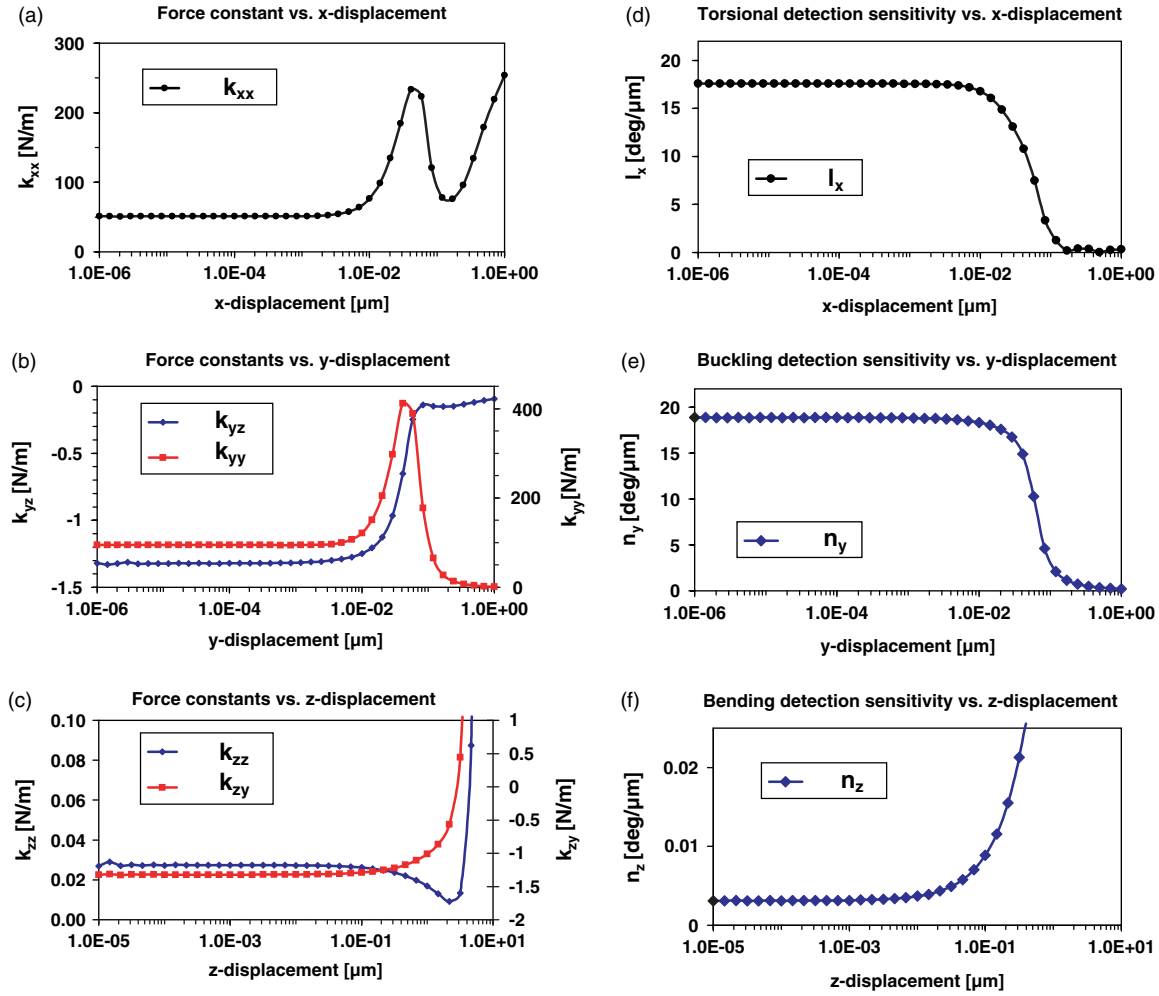

Figure 5. Nontrivial force constants and relative detection sensitivities as a function of tip displacements calculated by FE analysis. The calculated parameters are nearly constant for small displacements of the tip. For high displacements, strong nonlinearities occur.

in the frame of reference of the cantilever (Fig. 4(a)) can be given in the form:

$$\overleftrightarrow{K} = \begin{pmatrix} k_{xx} & 0 & 0 \\ 0 & k_{yy} & k_{yz} \\ 0 & k_{zy} & k_{zz} \end{pmatrix}, \vec{\xi}_{\mathrm{NFM}} = \begin{pmatrix} 0 \\ n_y \\ n_z \end{pmatrix}, \vec{\xi}_{\mathrm{LFM}} = \begin{pmatrix} l_x \\ 0 \\ 0 \end{pmatrix} \quad (2)$$

where $k_{yz} = k_{zy}$.

For the Microlever C considered here, the FE analysis gives the following results:

$$\overleftrightarrow{K} = \begin{pmatrix} 51.0 & 0 & 0 \\ 0 & 94.8 & -1.32 \\ 0 & -1.32 & 0.27 \end{pmatrix} [\mathrm{N/m}]$$

$$\vec{\xi}_{\mathrm{NFM}} = \begin{pmatrix} 0 \\ 18.7 \\ 0.003 \end{pmatrix} [\mathrm{deg/\mu m}]$$

$$\vec{\xi}_{\mathrm{LFM}} = \begin{pmatrix} 17.4 \\ 0 \\ 0 \end{pmatrix} [\mathrm{deg/\mu m}] \quad (3)$$

It is remarkable that on the one hand the values for the lateral components k_{xx} and k_{yy} of the force constant matrix are two orders of magnitude higher than the corresponding values of the normal component k_{zz}. On the other hand, since relative detection sensitivities for tip displacements in the lateral directions are more than three orders of magnitude higher than those in the normal direction, the relative detection sensitivities for lateral forces are even higher than those for normal forces. The nondiagonal elements of the force constant matrix are a measure of the coupling between bending and buckling and are of special importance for operating modes of the AFM in which the coupling between y and z direction is not negligible.

Apart from calculations for cantilever type C described above, the corresponding calculations have also been performed for other cantilevers with different geometries (Microlever type D, E and F). The results qualitatively agree with the data mentioned above. Table 1 lists the cantilever data we obtained from the analysis, together with the parameters used in our FE model.

Method for the determination of parameters for individual cantilevers

For the FE calculations shown above, typical values for the mechanical properties of shell elements representing the cantilever beam were used. However, as mentioned above, especially the Young's modulus E and the thickness t, which are not easy to obtain experimentally, vary over a wide range, particularly for cantilevers of different wafers. For that reason, the values of the calculated force constants

DOI: 10.1002/sia

exhibit a relatively large uncertainty of more than a factor of 2. Therefore, it is of interest to be able to calculate the force constants of individual cantilevers with their specific properties. All components of the force constants are proportional to $E \times t^3$. For this reason, it is possible to eliminate the scaling factor $E \times t^3$ by experimentally measuring one of these values – e.g. the bending force constant – in order to rescale all elements of the force constant matrix. In the literature, several publications deal with the experimental determination of the bending force constant of the cantilever.[17–19] In contrast to methods for measuring lateral force constants,[16,20] some of these methods for investigation of the bending force constant of the cantilever are easy to perform.[17,18] Since $E \times t^3$ varies only slightly between neighboring cantilever chips within the same wafer, it may be sufficient to measure only the force constants of a few different cantilevers at certain distances.[19]

CONCLUSIONS

In summary, using a parameterized FE model, force constants and detection sensitivities for different cantilever geometries were calculated. The resulting data are essential for the interpretation and the quantitative evaluation of a wide range of AFM measurements. Lateral forces of cantilevers with respect to the surface-sticking tip (e.g. for investigation of friction effects and tip-induced wear) as well as lateral tip displacements due to normal modulation could be estimated. The latter are of high relevance e.g. for FMM measurements. Other applications of the calculated data include the removal of artifacts due to lateral forces in topographic images.

It was shown that within the limits typical for many AFM measurements the cantilevers show a linear bending behavior as a function of tip displacement according to Hook's law in each spatial direction. Thus, the FE model results are applicable for different frames of reference in an easy manner.

REFERENCES

1. Mayer G, Amer NM. *Appl. Phys. Lett.* 1990; **56**: 2100.
2. Maivald P, Butt HJ, Gould SA, Prater CB, Drake B, Gurley JA, Elings VB, Hansma P. *Nanotechnology* 1991; **2**: 103.
3. Rabe U, Kester E, Arnold W. *Surf. Interface Anal.* 1999; **27**: 386.
4. Pfrang A, Send W, Gerthsen D, Schimmel Th. *Surf. Interface Anal.* 2002; **33**: 96.
5. Kemnitzer R, Koch Th, Küppers J, Lux-Steiner M, Schimmel Th. In *Fundamentals of Triobology and Bridging the Gap between the Macro- and Micro/Nanoscales, (NATO-ASI Series)*, Bhushan B (ed.). Kluwer Academic Publishers: Dordrecht, 2001; 495.
6. Müller M, Fiedler Th, Schimmel Th. In *Fundamentals of Triobology and Bridging the Gap between the Macro- and Micro/Nanoscales*, (NATO-ASI Series), Bhushan B (ed.). Kluwer Academic Publishers: Dordrecht, 2001; 487.
7. Feiler A, Attard P, Larson I. *Rev. Sci. Instrum.* 2000; **71**: 2746.
8. Sader JE, White LR. *J. Appl. Phys.* 1993; **74**: 1.
9. Butt HJ, Siedle P, Seifert K, Fendler K, Seeger T, Bamberg E, Weisenhorn AL, Goldie K, Engel A. *J. Microsc.* 1993; **169**: 75.
10. Sader JE. *Rev. Sci. Instrum.* 1995; **66**: 4583.
11. Noy A, Frisbie CD, Rozsnyai LF, Wrighton MS, Lieber CM. *J. Am. Chem. Soc.* 1995; **117**: 7943.
12. Hazel JL, Tsukruk VV. *Thin Solid Films* 1999; **339**: 250.
13. Neumeister JM, Ducker WA. *Rev. Sci. Instrum.* 1994; **65**: 2527.
14. Warmack RJ, Zheng XY, Thundat T, Allison DP. *Rev. Sci. Instrum.* 1994; **65**: 394.
15. Sader JE. *Rev. Sci. Instrum.* 2003; **74**: 2438.
16. Sader JE, Sader RC. *Appl. Phys. Lett.* 2003; **83**: 3195.
17. Gibson CT, Watson GS, Myhra S. *Nanotechnology* 1996; **7**: 259.
18. Sader JE, Chron JW, Mulvaney P. *Rev. Sci. Instrum.* 1999; **70**: 3967.
19. Cleveland JP, Manne S, Bocek D, Hansma PK. *Rev. Sci. Instrum.* 1993; **64**: 403.
20. Green CP, Lioe H, Cleveland JP, Proksch R, Mulvaney P, Sader JE. *Rev. Sci. Instrum.* 2004; **75**: 1988.

DOI: 10.1002/sia